

Study and realization of an electrostatic precipitator device

Med Ali Kouidri*, D. Mahi

Laboratory of studies and Development of Semiconductor and Dielectric Materials, LeDMaScD, University Amar Telidji of Laghouat, Algeria

Corresponding Author Email: kouidrimedali@yahoo.fr

https://doi.org/10.18280/mmc_c.790415

ABSTRACT

Received: 18 February 2018

Accepted: 10 April 2018

Keywords:

Electro filter, corona discharge, geometry, electric field, ionization, particles, environment, high voltage

An electrostatic filter is a device consisting of plates (receiving electrodes) arranged vertically between which there vertically tensioned wires (electrodes) are electrically powered by the high voltage. A negative voltage applied to the emitting electrodes, generates the formation of electrons in the vicinity of these, which ionize the gas molecules. These ions are attracted by the collector plates and charge the dust by corona effect on their paths. These dusts are then attracted to the collector plates and adhere to it. Cleaning is provided by the Hammers striking regularly these plates allow to picking up the particles at regular intervals. The dust is thus collected to be evacuated. The obtained results of the different geometries showed that this aspect represents a dominant influence on the design and implementation of corona discharge reactor.

1. INTRODUCTION

Most industrial units located on fertile land in sensitive areas to pollution or appointed on ground water, are a threat to the living and the environment. Table 1 summarizes most of the polluting sources.

Therefore, filtering is one of remediation solutions. The treatment can be done using various materials [1-2]:

- Cyclones; Ventured scrubbers;
- The dust collectors filter media;
- Electrostatic precipitators.

Electrostatic precipitators are often used on industrial sites for the dust removal of flue gases and gases from flares and chimneys before they are released into the atmosphere. They are also used to recover valuable chemicals or metals

suspended in rejected gases that may have a market value and be reused. These devices use electric fields to move particles in the inter-electrode gap.

Various depollution techniques have been proposed and several theoretical and experimental works have been carried out to study this Phenomenon. They aim to propose mathematical models able to simulate the behavior of the electrostatic filter [3-4].

In this work, we propose a theoretical and practical study defining the geometric design of a high voltage electrostatic precipitator. It uses an emitter electrode negatively charged, ensuring the ionization of the particles moving, under the effect of the electric field, and are deposited on the collecting electrode.

Table 1. Major atmospheric emission sources [27]

Installation	Main pollutants expected
Gas turbine	CO, CO ₂ , NO _x , Volatile Organic Compounds (COV)
Torch	CO, CO ₂ , NO _x , COV
Lubrication oil events of the turbine	CH ₄ , CO, CO ₂ , NO _x , COV
Glycol boiler	CO, CO ₂ , NO _x , COV
Burn pit	CO, CO ₂ , NO _x , COV, carbonaceous particles

2. OPERATING PRINCIPLE OF THE REALIZED DEVICE

The experimental setup is carried out in the laboratory for the study and development of dielectric materials.

Its operating principle is based on electrostatic filtration, through the negatively charged emitting electrode (see Figure 1); the electrons are emitted and activated up to the positively

charged collector electrodes.

The particles flowing in the electro filter are negatively charged by the activated electrons where these ions deposited and move in the direction of the collecting electrode, and having as essential purpose the ionization depollution.

The following figure summarizes in detail of the electrostatic filtration mechanism already cited.

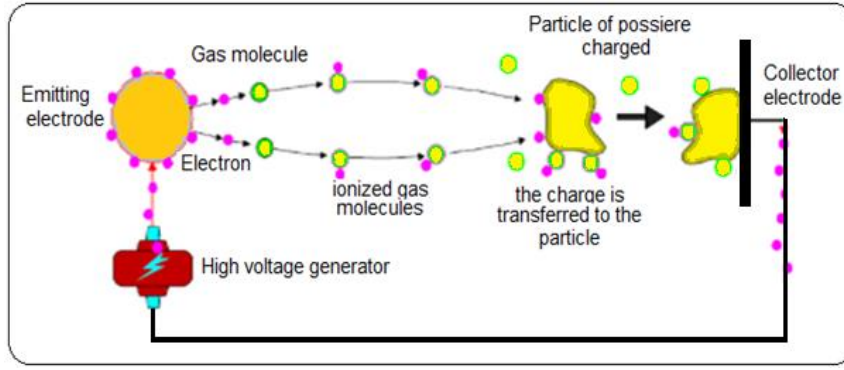


Figure 1. Mechanism for collecting pollution

3. AIR GAP RUPTURE MECHANISM

The geometrical form of (point-plane) electrode imposes a non-uniform field. The effective ionization coefficient $\bar{\alpha}$ varies along the inter-electrode interval, according to the following relationship [5-8]:

$$\bar{\alpha} = \alpha - \eta \quad (1)$$

where:

- α : The first Townsend ionization coefficient;
- η : The attachment coefficient.

For high pressures and non-uniform fields, the Townsend criterion (self-discharge) takes the form [9, 10].

$$\gamma \left(\exp \left(\int_0^h \bar{\alpha} \cdot dx \right) - 1 \right) = 1 \quad (2)$$

where:

- $\bar{\alpha}$: The effective ionization coefficient;
- γ : The second Townsend ionization coefficient;
- h : The inter-electrode distance.

The integral is usually calculated along the most intense field line. When the field reaches a critical value E_c , the integral $\int \bar{\alpha} dx$ ceases to exist, and the Townsend mechanism loses validity.

Consequently, the ionization phenomenon only appears in the region of the inter-electrode space, which satisfies the condition $\bar{\alpha} > 0$ [11-13].

The number of electrons at a distance "x" as below:

$$N(x) = N_0 \cdot e^{(\alpha \cdot x)} \quad (3)$$

If taking into account the non-uniform distribution then, the number of electrons is given by:

$$N_{cr} = \exp \left(\int_0^{x_c} \bar{\alpha} \cdot dx \right) \quad (4)$$

where: N_{cr} is the concentration of the critical charge in the avalanche giving an ionization level for the streamer propagation, x_c is the critical distance of the avalanche. Then equation (4) becomes:

$$\int_0^{x_c} \bar{\alpha} \cdot dx \geq k \quad (5)$$

where: x_c is the length of the avalanche from the high voltage electrode. The left side of this equation states that the effective ionization takes place in the field region where $0 \leq x \leq x_c$ with the condition $\bar{\alpha} > 0$; K is the number that takes into account any feedback process ($k = 18-20$) [14-18].

The modelling of electrostatic requires the calculation of the charge accumulated by the particles along their path. To do this use is made of the physical models that describe the charging process taking into account the specific conditions present in electrostatic precipitators.

Several studies [19-22] have shown that particle loading can be mainly attributed to two mechanisms:

- The charge per field
- The charge by diffusion.

Generally, the electric charge acquired by a particle is the consequence of the interactions between the charge and the ions resulting from the corona discharge. Both charging process simultaneously involved and their relative importance is determined primarily by the particle size and intensity of the electric field.

The calculation of the limit charge of the particles is mainly based on the theory developed by Pauthenier [23-24]. The temporal evolution of the charge for a particle located in an electric field E , is described by the following expression given by White [19]:

$$\frac{dq_p}{dt} = \frac{\rho \cdot \mu \cdot q_p^s}{4 \cdot \epsilon_0} \cdot \left(1 - \frac{q_p}{q_p^s} \right)^2; \text{ for } q_p < q_p^s \quad (6)$$

In which ρ represents the ion density and μ is the ion mobility. The charge limit for the field is given by the following expression [19]:

$$q_p^s = 3 \cdot \pi \cdot \epsilon_0 \cdot \frac{\epsilon_r}{\epsilon_r + 2} \cdot E \cdot d_p^2 \quad (7)$$

where ϵ_r is the relative permittivity of the particles. We find in equation (7) that the limit charge per field is a function of the intensity of the local electric field, the relative permittivity ϵ_r of particles q_p is obtained by the integration over time of equation (6). In the particular case where the

distributions of the electric field and the ion space charge are homogeneous, the integration of the relation (7) gives us:

$$q_p(t) = q_p^s \cdot \left(\frac{t}{t + \tau_p} \right)$$

With $\tau_p = \frac{4 \cdot \epsilon_0}{\rho \cdot \mu}$ (8)

where τ_p is the characteristic charge time per field and represents the time at which the charge of the particle reaches half of the limit charge. In the case of electrostatic precipitators, the intensity of the electric field and the density of ions vary in the inter-electrode space; the value of the limit charge will therefore be specific for each position of the particles.

Pauthenier, Cochet [22] have proposed a simple expression that allows the calculation of the limit charge for fine particles of comparable size to the average free path of the ions. This relation (9), which involves the ratio λ_g/d_p , represents a simple means of calculating the saturation charge, while offering a good accuracy for particles with a diameter greater than 0,1 μm [25].

$$q_p^s = \left[\left(1 + \frac{2\lambda_g}{d_p} \right)^2 + \left(\frac{2}{1 + 2 \cdot \frac{\lambda_g}{d_p}} \right) \cdot \left(\frac{\epsilon_{r-1}}{\epsilon_{r+2}} \right) \right] \cdot \pi \cdot \epsilon_0 \cdot d_p^2 \cdot E$$
 (9)

where: λ_g is the average free path of the gas molecules can be estimated by:

$$\lambda_g = \frac{\mu_g}{0.499 \cdot \rho_g} \cdot \sqrt{\frac{\pi \cdot M}{8 \cdot R \cdot T}}$$
 (10)

where: M is the molar mass; R is the universal constant of perfect gases (8.31 J/K.mol) and (T) absolute temperature. Under normal conditions of temperature and pressure, the average free path of the ions is $\lambda_g = 6.53 \times 10^{-8} (m)$.

As for the diffusion charge, it concerns very fine particles, with a diameter of less than 0.2 μm . In the charge by diffusion, the accumulated charge quantity depends on the particle size, the density of the ions, the average rate of thermal agitation of the ions, the dielectric constant of the particle, the absolute temperature of the gas and the time of presence of the particles within the field. White [19] shows that the evolution over time of the charge acquired by a particle under the effect of the diffusion process is given by:

$$\frac{d \cdot q_p}{dt} = \frac{\pi \cdot d_p^2}{4} \cdot V_1 \cdot \rho \cdot \exp\left(\frac{q_p \cdot e}{2 \cdot \pi \cdot \epsilon_0 \cdot d_q \cdot k \cdot T} \right)$$

With $V_1 = \sqrt{\frac{3 \cdot k_B \cdot T}{m_i}}$ (11)

where: $k_B = 1.38 \times 10^{-23} \text{ J / k}$ represents the Boltzmann constant; V_1 is the thermal stirring speed of the ions and with

m_i the mass of the ion. Considering a density of ions ρ uniform, expression (11) after integration leads to:

$$q_p(t) = q^* \cdot \ln\left(1 + \frac{t}{\tau_d} \right)$$

With $q^* = 2 \cdot \pi \cdot \epsilon_0 \cdot d_p \cdot T \cdot k_B / e$ (12)

The diffusion charge constant is given by:

$$\tau_d = 8 \cdot \epsilon_0 \cdot k_B \cdot T / d_p \cdot v_i \cdot \rho \cdot e$$
 (13)

where: τ_d is the characteristic time of charge by diffusion. We observe that equation (12) does not lead to a limit charge for τ to infinity. However, the expression (11) shows that the diffusion charging process is continuously influenced by the charge d_p already acquired by the particle. The corona effect can be adequately described with the equations governing a unipolar ion drift zone:

$$E = -\nabla\Phi = -\text{grad}\Phi$$
 (14)

$$\nabla^2\Phi = \text{div}\text{grad}\Phi = \frac{\rho}{\epsilon_0}$$
 (15)

$$j = \rho \cdot v = \rho \cdot \mu \cdot E$$
 (16)

$$\nabla \cdot j = \text{div}j = 0$$
 (17)

where:

E : The electric field.

Φ : The potential.

ρ : The density of the electric charge.

j : The current density.

v : The speed of ions.

μ : The movement of ions.

ϵ_0 : The permittivity of the vacuum.

The density of the electric charge ρ includes the charge by ion diffusion and the charges accumulated by the solid particles.

4. SIMULATION OF THE EXPERIMENTAL DEVICE

We have modeled the fields and potentials electrostatic by the finite element method on a triangular mesh. A simulation performed using the COMSOL multi-physics software version 3.5b [26]. The results obtained in terms of field and potential in the inter-electrode space taking into account the influence of the inter-electrode distance (h), the spacing between points (d) and the radius of curvature (r).

4.1 Geometry point-plan

In this configuration the field of study is discretise using triangular elements linear. It is shown in Figure 2.

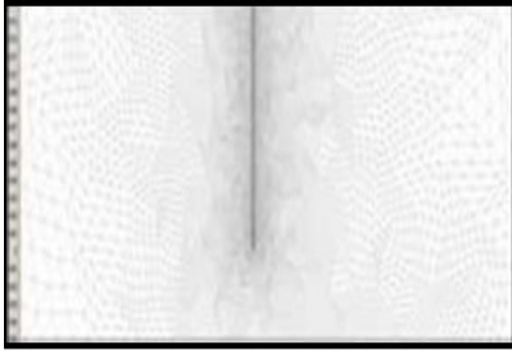
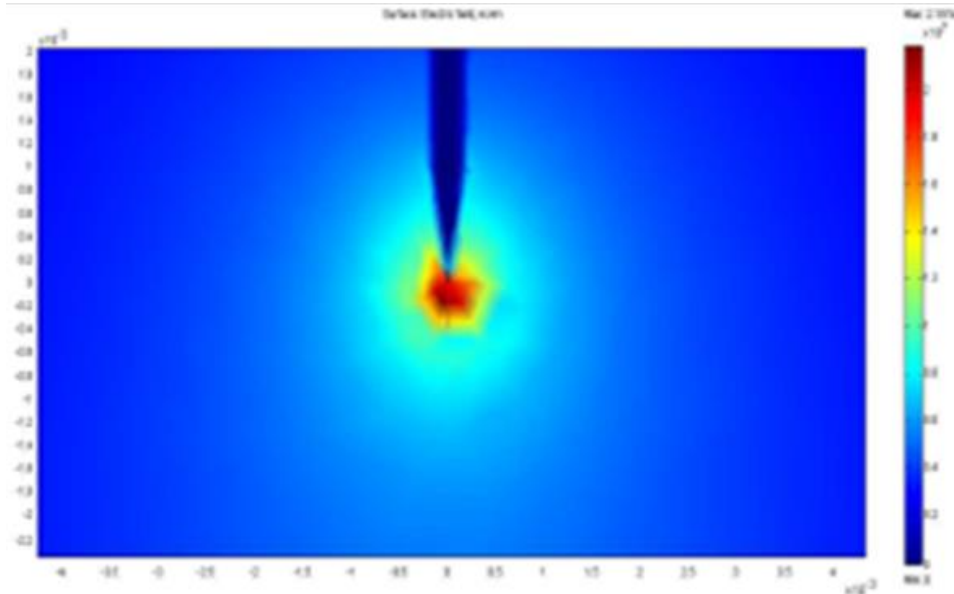


Figure 2. Mesh of the peak-plane domain

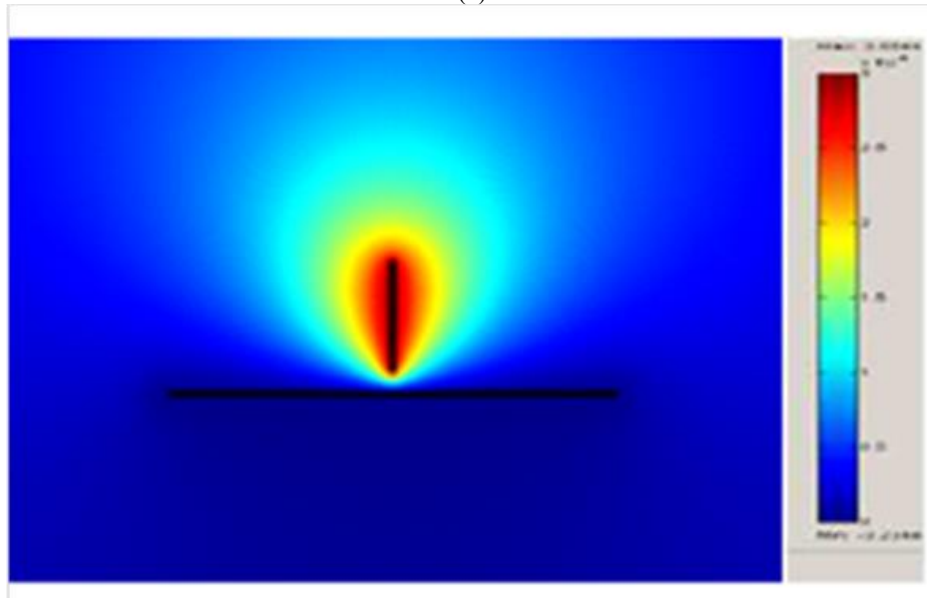
4.1.1 Influence of the inter-electrode distance (h)

The inter-electrode distance is an important factor for control the repartition of the electric field and the potential in the inter-electrode space. Care must be taken to avoid the breakdown of the interval (electrical arc). We know that for the same inter-electrode distance, the breakdown voltage is higher than negative voltage to positive voltage. Figures 3 (a) and 3 (b) illustrate the distribution of the electrical potential at the head and around the high voltage electrode.

Figures 4 (a) and 4 (b) show the variations of the potential and field distribution for several values of the inter-electrode distance (h) 5, 10, 15 and 20mm, and an applied voltage equal to 30kV.



(a)



(b)

Figure 3. Range of potential distributed around the point electrode.

(a): On the point of the electrode

(b): Around the electrode

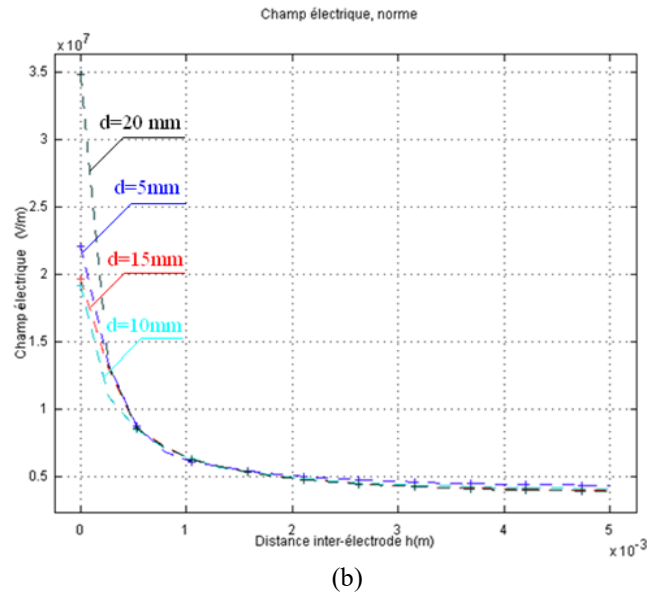
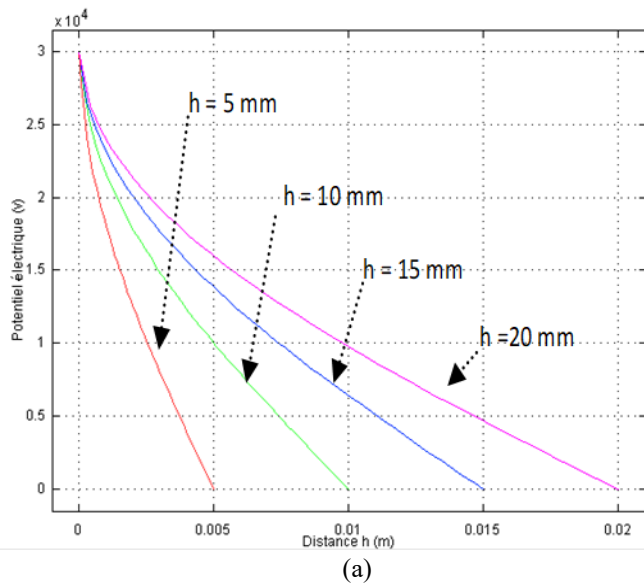


Figure 4. Potential and electric field along the axis between electrodes for different (h).
 (a): On the point of the electrode (b): Around the electrode

4.1.2 Influence of the radius of curvature

The radius of curvature, r , of reference taken in this study is 2 mm. Figure 5 show the variations of the electric field for several values of r . The results show that the electric field reaches a maximum value, which decreases as the radius of curvature of the point increases.

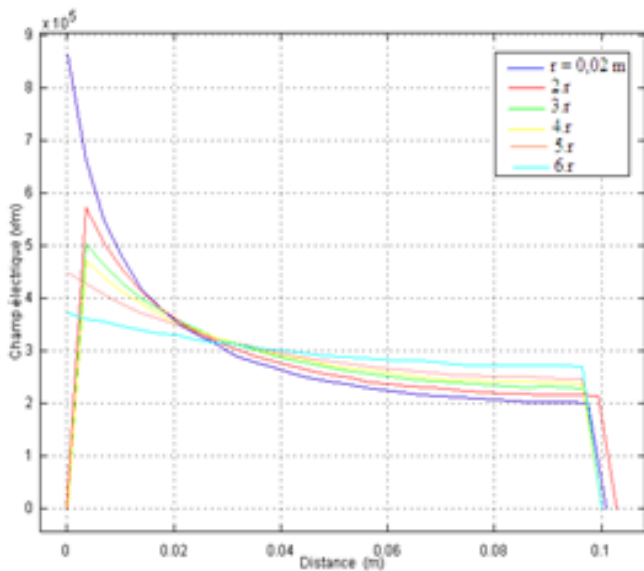


Figure 5. Electric field for different radius of curvature (r , $2r$, $3r$, $4r$, $5r$, $6r$)

4.2 Influence of the number of points

4.2.1 Case of three points

In order to study the influence of the adjacent electrodes on the central electrode, a number of electrodes equal to three, spaced 5 mm apart were chosen. The contiguous points may influence the value of the electric field. The domain discretization is shown in Figure 6.

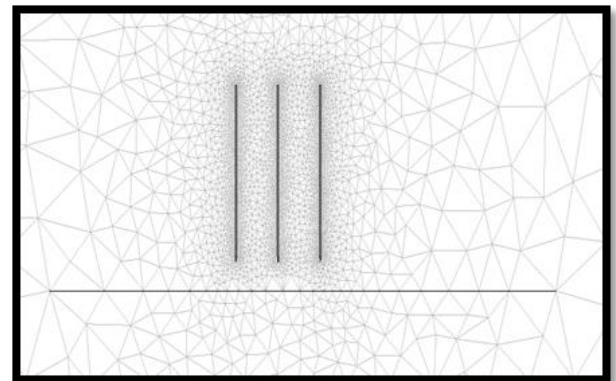


Figure 6. Mesh of the domain of 3 electrodes-plane

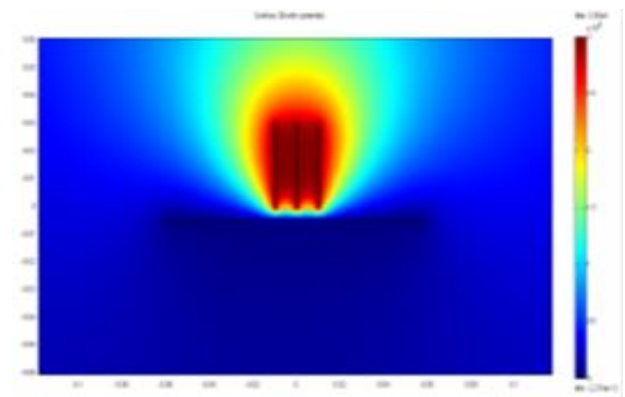


Figure 7. Variation of the electric field around the electrodes

We find that the values of the electric field and the potential evolve between a maximum value at each point is a minimum value when approaching the plane electrode. It should be noted that beyond a certain inter-electrode distance, the value of the electric field is not influenced. Figure 7 shows the distribution of the electrical potential between and around the three point-plane electrodes.

4.2.2 Multi-point - Plan case

The objective of multiplying the number of electrode points, having the same characteristics, is to obtain an intense field and a high efficiency of the experimental device. The simulations are performed for a number of points equal to 31, because the experimental device makes it possible to receive a number of electrodes equal to 31 points. The discretization of the domain is show in Figure 8.

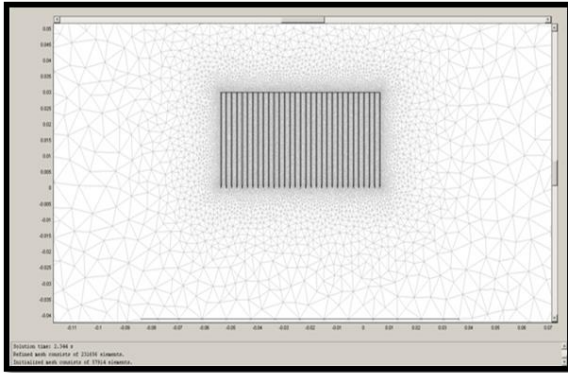
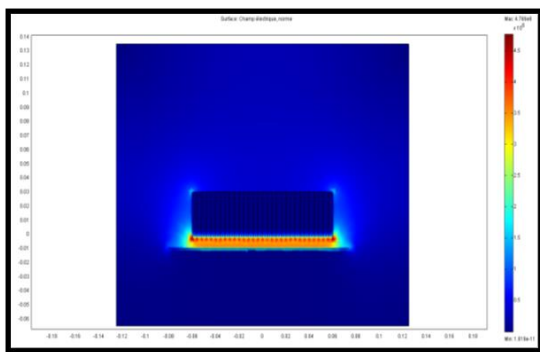


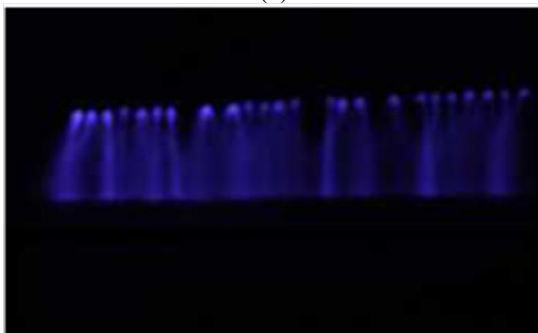
Figure 8. Mesh of the Multi-point structure

Figure 9 (a) shows the distribution of the electrical potential around the multi-point-plane electrodes. We observe certain homogeneity of the electric field and that the field lines in the inter-electrode space are uniform. There is no more interaction between the points.

Figure 9 (b) shows the photographs of the discharges obtained on the experimental device. There is a uniform glow of pre-discharges with two zones: One, bright around the high-voltage electrode and a second, ahead of the first, of lower intensity. We also note that the radius of the light channel is not uniform, along the path of the latter.



(a)



(b)

Figure 9. The pace of the electric shock.
(a): Simulation result. (b): Experimental result photography

The Fig. 9 (a) illustrate the simulation of electrical field of the multi-points Plan configuration, we noticed that the simulate electric field in this case is intense. Thus increasing the efficiency of electrostatics precipitation, that is what it shows in experimental discharge Fig. 9 (b) that the plasma between the electrodes occupies all the space, which means a sufficient intensity of field to ionize the particles. The obtained simulations of the electric field share some common features with the existing experimental results about the electric field efficiency.

5. CONCLUSION

This work focused on the study of a multi-point - plan device. It emerges from a study that the influential parameters that must be considered when designing the corona reactor:

As a global conclusion of all the results obtained, we could say that the inter-electrode distance h and the radius of curvature of the high voltage electrode r influence the distribution of the potential and the electric field in the inter-electrode interval. The value of the electric field increases exponentially when h decreases, on the other hand, the electric field decreases as the radius of curvature of the high voltage electrode increases.

For the case of the multi-point electrodes, we noticed that the approach of the points acts in favour of the interferences of the field lines leading to a net decrease of the electric field, in particular, for the electrodes of the medium. The distance (d) beyond a certain value equal to 5 times h , proves necessary.

As for the corona discharge zone, we notice that from a certain value of the applied voltage (V) to the point, and for each value of the inter-electrode distance, an increase in the radius of curvature leads to a significant decrease of the electric field and that the latter is inversely proportional to the radius of curvature.

The results obtained have shown that, the multi-point plane configuration makes it possible to have a homogeneous spatial distribution of the electric field with a concentration of the field lines at the points. However, it is found that the multiplication of the number of points, with a small radius of curvature and an inter-electrode distance as small as it allows having an almost homogeneous distribution of the field lines. This improves the efficiency and performance of electro filters.

A concordance of the results obtained between experimentation and simulation, which explains the physical understanding of the phenomena treated in this study.

REFERENCES

- [1] Eglin T. (2012). Agricultural emissions of particles in the air. State of play and levers of action. ADEME, Agency for the Environment and Energy Management, p. 34.
- [2] Benamar B. (2008). The reliability of the electro filtration of a dust charge atmosphere. PhD thesis of Henri Poincare University. Nancy1, France.
- [3] Adamiak K. (2013). Numerical models in simulating wire-plate electrostatic precipitators. A review, Journal of Electrostatics 71(4): 673-680.

- <https://doi.org/10.1016/j.elstat.2013.03.001>
- [4] Dein E, Usama K. (2014). Experimental and simulation study of V–I characteristics of wire–plate electrostatic precipitators under clean air conditions. *Arab J Sci Eng* 39(5): 4037–4045. <https://doi.org/10.1007/s13369-014-1046-2>
- [5] Guillaume D, Benoît F. (2004). Crown discharge, applications and modeling. *Industrial Energetics ESIP*.
- [6] Vincent A. (2002). Design and simulation of a wire-cylinder corona discharge reactor with dielectric barrier adapted to the treatment of nitrogen oxides in effluents marked by an isotope. Doctoral Thesis of The University of Pierre and Marie curie Paris VI.
- [7] Sigmond RS, Goldman M. (1989). Corona discharge physics and applications, breakdown and discharges in gases - Part B. NATO ASI series B89-B.
- [8] Gary C, Moreau M. (1976). The corona effect in alternating voltage. Editions Eyrolles (Paris), pp. 17-33, 283-302.
- [9] Jordan JB. (1966). Foul weather corona. Research Report, Electrical Engineering Department, Laval University, Québec.
- [10] Farzaneh M. (1986). Contribution to the study of the mechanisms of the vibrations induced by the effect of crown. Thesis of Doctorate of State, Presented to The University Paul Sabatier of Toulouse.
- [11] Giao TN, Jordan JB. (1968). Modes of corona discharge in air. *IEEE Transactions PAS-87(5)*: 1207-1215. <https://doi.org/10.1109/TPAS.1968.292211>
- [12] Phan LC, Farzaneh M. (1989). Course notes high voltage. University of Chicoutimi, Canada.
- [13] Jean-Charles Matéo-Vélez. (2006). Modeling and numerical simulation of plasma generation in crown discharges and its interaction with aerodynamics. PhD thesis, University of Toulouse, ONERA.
- [14] Massines F. (2004). Cold plasmas, Generation, Characterization and Technologies. Publications of the University of Saint-Etienne.
- [15] Goldman M. (1978). Cold plasmas at atmospheric pressure. *Plasmas in Industry*, Dopée Coll., Ed. Electra, Paris.
- [16] Nasser E. (1971). Fundamentals of gaseous ionization and plasma electronics. Wiley– Inter-Sciences.
- [17] Gallimberti I. (1972). A computer model for streamer propagation. *J. Phys. D: Appl. Phys* 5: 2179-2189. <https://doi.org/10.1088/0022-3727/5/12/307>
- [18] Lachaud S. (2002). Point-to-plane discharge in gaseous mixtures corresponding to industrial effluents: electrical and physicochemical study, application to the destruction of nitrogen dioxide. Thesis UPPA,
- [19] White HJ. (1963). Industrial electrostatic precipitation. Addison Wesley Publishing Company, New York.
- [20] Egli W, Riccius O, Kogelschatz U, Gruber R, Merazzi S. (1994). Computation of the charge density distribution in a 3D electric field. 6th Joint EPS-APS Intern. Conf. On Physics Computing (PC'94), Lugano, pp. 535-542.
- [21] Egli W, Kogelschatz U. (1995). Corona current and space charge distribution in precipitator configurations. XXII Intern. Conf.on Phenomena in Ionized Gases, (ICPIG XXII), Hoboken, NJ 1: 119-120.
- [22] Porle K, Parker KR. (1997). Dry type precipitator applications in applied electrostatic precipitation. Blackie Academic & Professional, London, pp. 349-381.
- [23] White HJ. (1965). Industrial electrostatic precipitation. Addison-Wesley.
- [24] Leonard G, Mitchner M, Self SA. (1980). Particle transport in electrostatic precipitators. *Atmospheric Environ* 14(11): 1289-1299. [https://doi.org/10.1016/0004-6981\(80\)90230-9](https://doi.org/10.1016/0004-6981(80)90230-9)
- [25] Parker KR. (1997). Electrostatic precipitation, Chapman & hall, pp. 1-24.A.
- [26] Djekidel R, Mahi D. (2014). Effect of the shield lines on the electric field intensity around the high voltage overhead transmission lines. *AMSE Journals, Series Modelling. A* 87(1): 1-16.
- [27] Ali KM, Mahi D, Hadjadj A. (2015). Contribution to the depollution of the elements ejected by an energy production with the application of electro filter high voltage: Design of Electro filter multi-compartment. *Electrical Engineering (ICEE)*, 4th International Conference on. IEEE. <https://doi.org/10.1109/INTEE.2015.7416674>